

On Extended Long Short-term Memory and Dependent Bidirectional Recurrent Neural Network

Yuanhang Su^{a,*}, Yuzhong Huang^a, C.-C. Jay Kuo^a

^a*University of Southern California, Ming Hsieh Department of Electrical Engineering, 3740 McClintock Avenue, Los Angeles, CA, United States*

Abstract

In this work, we investigate the memory capability of recurrent neural networks (RNNs), where this capability is defined as a function that maps an element in a sequence to the current output. We first analyze the system function of a recurrent neural network (RNN) cell, and provide analytical results for three RNNs. They are the simple recurrent neural network (SRN), the long short-term memory (LSTM), and the gated recurrent unit (GRU). Based on the analysis, we propose a new design to extend the memory length of a cell, and call it the extended long short-term memory (ELSTM). Next, we present a dependent bidirectional recurrent neural network (DBRNN) for the sequence-in-sequence-out (SISO) problem, which is more robust to previous erroneous predictions. Extensive experiments are carried out on different language tasks to demonstrate the superiority of our proposed ELSTM and DBRNN solutions.

Keywords: recurrent neural networks, long short-term memory, gated recurrent unit, bidirectional recurrent neural networks, convolutional sequence to sequence, natural language processing

1. Introduction

The recurrent neural network (RNN) has proved to be an effective solution for natural language processing (NLP) through the advancement in the last

*Corresponding Author
Email address: suyuanhang@hotmail.com

three decades [1, 2]. At the cell level, the long short-term memory (LSTM) [3] and the gated recurrent unit (GRU) [4] are often adopted by an RNN as its low-level building element. Built upon these cells, various RNN models have been proposed to solve the SISO problem. To name a few, there are the bidirectional RNN (BRNN) [5], the encoder-decoder model [4, 6, 7, 8] and the deep RNN [9].

LSTM and GRU cells were designed to enhance the memory length of RNNs and address the gradient vanishing/exploding issue [3, 10, 11], yet thorough analysis on their memory decay property is lacking. The first objective of this research is to analyze the memory length of three RNN cells - simple RNN (SRN) [1, 2], LSTM and GRU. It will be conducted in Sec. 2. Our analysis is different from the investigation of gradient vanishing/exploding problem in the following sense. The gradient vanishing/exploding problem occurs in the training process while memory analysis is conducted on a trained RNN model. Based on the analysis, we further propose a new design in Sec. 3 to extend the memory length of a cell, and call it the extended long short-term memory (ELSTM).

As to the macro RNN model, one popular choice is the BRNN [5]. Since elements in BRNN output sequences should be independent of each other, the BRNN cannot be used to solve dependent output sequence problem alone. Nevertheless, most language tasks do involve dependent output sequences. Another choice is the encoder-decoder system, where the attention mechanism was introduced to improve its performance in [7, 8]. We show that the encoder-decoder system is not an efficient learner by itself. A better solution is to exploit the encoder-decoder and the BRNN jointly so as to overcome their individual limitations. Following this line of thought, we propose a new multi-task model, called the dependent bidirectional recurrent neural network (DBRNN), in Sec. 4.

To demonstrate the performance of the DBRNN model with the ELSTM cell, we conduct a series of experiments on the part of speech (POS) tagging and the dependency parsing (DP) problems in Sec. 5. Finally, concluding remarks are given and future research direction is pointed out in Sec. 6.

2. Memory Analysis of SRN, LSTM and GRU

For a large number of NLP tasks, we are concerned with finding semantic patterns from input sequences. It was shown by Elman [1] that an RNN builds an internal representation of semantic patterns. The memory of a cell characterizes its ability to map input sequences of certain length into such a representation. Here, we define the memory as a function that maps elements of the input sequence to the current output. Thus, the memory of an RNN is not only about whether an element can be mapped into the current output but also how this mapping takes place. It was reported by Gers *et al.* [12] that an SRN only memorizes sequences of length between 3-5 units while an LSTM could memorize sequences of length longer than 1000 units. In this section, we conduct memory analysis on SRN, LSTM and GRU cells.

2.1. Memory of SRN

For ease of analysis, we begin with Elman’s SRN model [1] with a linear hidden-state activation function and a non-linear output activation function since such a cell model is mathematically tractable while its performance is equivalent to Jordan’s model [2] and Tensorflow variations.

The SRN model can be described by the following two equations:

$$c_t = W_c c_{t-1} + W_{in} X_t, \tag{1}$$

$$h_t = f(c_t), \tag{2}$$

where subscript t is the time unit index, $W_c \in \mathbb{R}^{N \times N}$ is the weight matrix for hidden-state vector $c_{t-1} \in \mathbb{R}^N$, $W_{in} \in \mathbb{R}^{N \times M}$ is the weight matrix of input vector $X_t \in \mathbb{R}^M$, $h_t \in \mathbb{R}^N$ in the output vector, and $f(\cdot)$ is an element-wise non-linear activation function. Usually, $f(\cdot)$ is a hyperbolic-tangent or a sigmoid function. Throughout this paper, we omit the bias terms by including them in the corresponding weight matrices. The multiplication between two equal-sized vectors in this paper is element-wise multiplication.

By induction, c_t can be written as

$$c_t = W_c^t c_0 + \sum_{k=1}^t W_c^{t-k} W_{in} X_k, \quad (3)$$

where c_0 is the initial internal state of the SRN. Typically, we set $c_0 = \underline{0}$. Then, Eq. (3) becomes

$$c_t = \sum_{k=1}^t W_c^{t-k} W_{in} X_k. \quad (4)$$

Let λ_{\max} be the largest singular value of W_c . Then, we have

$$\|W_c^{t-k} X_k\| \leq \|W_c\|^{t-k} \|X_k\| = \lambda_{\max}^{t-k} \|X_k\|. \quad (5)$$

Here, we are only interested in the case of memory decay when $\lambda_{\max} < 1$. Since the contribution of X_k , $k < t$, to output h_t decays at least in form of λ_{\max}^{t-k} , we conclude that SRN's memory decays exponentially with its memory length $|t - k|$.

2.2. Memory of LSTM

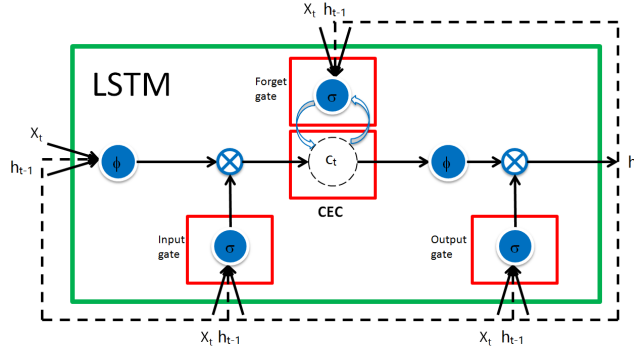


Figure 1: The diagram of a LSTM cell.

By following the work of Hochreiter *et al.* [3], we plot the diagram of the LSTM cell in Fig. 1. In this figure, ϕ , σ and \otimes denote the hyperbolic tangent function, the sigmoid function and the multiplication operation, respectively. All of them operate in an element-wise fashion. The LSTM cell has an input

gate, an output gate, a forget gate and a constant error carousel (CEC) module.

Mathematically, the LSTM cell can be written as

$$c_t = \sigma(W_f I_t) c_{t-1} + \sigma(W_i I_t) \phi(W_{in} I_t), \quad (6)$$

$$h_t = \sigma(W_o I_t) \phi(c_t), \quad (7)$$

where $c_t \in \mathbb{R}^N$, column vector $I_t \in \mathbb{R}^{(M+N)}$ is a concatenation of the current input, $X_t \in \mathbb{R}^M$, and the previous output, $h_{t-1} \in \mathbb{R}^N$ (i.e., $I_t^T = [X_t^T, h_{t-1}^T]$). Furthermore, W_f , W_i , W_o and W_{in} are weight matrices for the forget gate, the input gate, the output gate and the input, respectively.

Under the assumption $c_0 = \underline{0}$, the hidden-state vector of the LSTM can be derived by induction as

$$c_t = \sum_{k=1}^t \underbrace{\left[\prod_{j=k+1}^t \sigma(W_f I_j) \right]}_{\text{forget gate}} \sigma(W_i I_k) \phi(W_{in} I_k). \quad (8)$$

By setting $f(\cdot)$ in Eq. (2) to the hyperbolic-tangent function, we can compare outputs of the SRN and the LSTM below:

$$h_t^{SRN} = \phi \left(\sum_{k=1}^t W_c^{t-k} W_{in} X_k \right), \quad (9)$$

$$h_t^{LSTM} = \sigma(W_o I_t) \phi \left(\sum_{k=1}^t \underbrace{\left[\prod_{j=k+1}^t \sigma(W_f I_j) \right]}_{\text{forget gate}} \sigma(W_i I_k) \phi(W_{in} I_k) \right). \quad (10)$$

We see from the above that W_c^{t-k} and $\prod_{j=k+1}^t \sigma(W_f I_j)$ play the same memory role for the SRN and the LSTM, respectively.

If W_f in Eq. (10) is selected such that

$$\min |\sigma(W_f I_j)| \geq \lambda_{\max}, \quad \forall \lambda_{\max} \in [0, 1),$$

then

$$\left| \prod_{j=k+1}^t \sigma(W_f I_j) \right| \geq \lambda_{\max}^{|t-k|}. \quad (11)$$

As given in Eqs. (5) and (11), the impact of input I_k on the output of the LSTM lasts longer than that of the SRN. This is the case if an appropriate weight matrix, W_f , of the forget gate is selected.

2.3. Memory of GRU

The GRU was originally proposed for neural machine translation [4]. It provides an effective alternative for the LSTM. Its operations can be expressed by the following four equations:

$$z_t = \sigma(W_z X_t + U_z h_{t-1}), \quad (12)$$

$$r_t = \sigma(W_r X_t + U_r h_{t-1}), \quad (13)$$

$$\tilde{h}_t = \phi(W X_t + U(r_t \otimes h_{t-1})), \quad (14)$$

$$h_t = z_t h_{t-1} + (1 - z_t) \tilde{h}_t, \quad (15)$$

where X_t , h_t , z_t and r_t denote the input, the hidden-state, the update gate and the reset gate vectors, respectively, and W_z , W_r , W , are trainable weight matrices. Its hidden-state is also its output, which is given in Eq. (15). By setting U_z , U_r and U to zero matrices, we can obtain the following simplified GRU system:

$$z_t = \sigma(W_z X_t), \quad (16)$$

$$\tilde{h}_t = \phi(W X_t), \quad (17)$$

$$h_t = z_t h_{t-1} + (1 - z_t) \tilde{h}_t. \quad (18)$$

For the simplified GRU with the initial rest condition, we can derive the following by induction:

$$h_t = \sum_{k=1}^t \left[\underbrace{\prod_{j=k+1}^t \sigma(W_z X_j)}_{\text{update gate}} \right] (1 - \sigma(W_z X_k)) \phi(W X_k). \quad (19)$$

By comparing Eqs. (8) and (19), we see that the update gate of the simplified GRU and the forget gate of the LSTM play the same role. One can control the memory decay behavior of the GRU by choosing the weight matrix, W_z , of the update gate carefully.

3. Extended Long Short-Term Memory (ELSTM)

As discussed above, the LSTM and the GRU have longer memory lengths by introducing the forget and the update gates, respectively. However, from Eqs.

(10) and (11), we see that the impact of the proceeding element to the current output at time step t still decays quickly. However, this does not have to be the case. To demonstrate this point, we will present a new model and call it the extended long short-term memory (ELSTM) in this section. In particular, we propose the following two ELSTM cells:

- ELSTM-I: the ELSTM with trainable input scaling vectors $s_i \in \mathbb{R}^N$, $i = 1, \dots, t-1$, where s_i and s_j (with $i \neq j$) are independent.
- ELSTM-II: the ELSTM-I with no forget gate.

They are depicted in Figs. 2 (a) and (b), respectively.

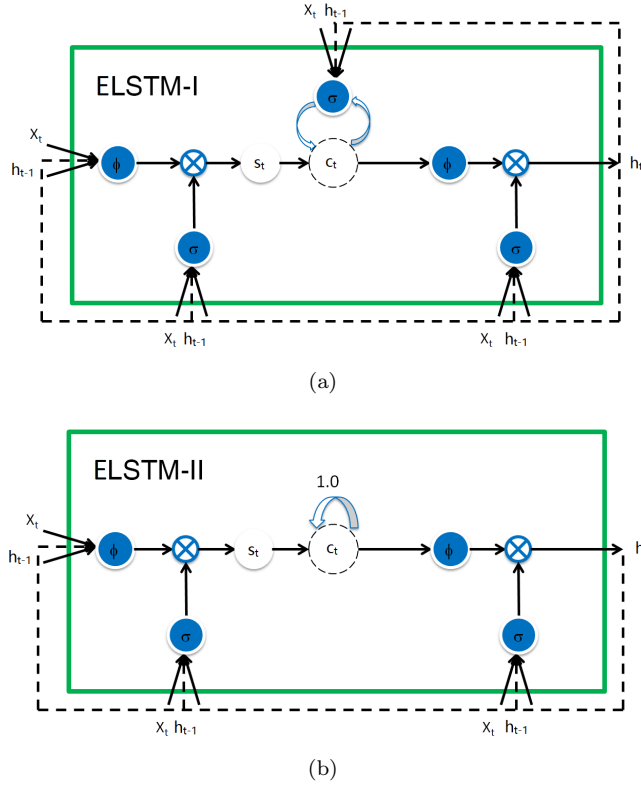


Figure 2: The diagrams of (a) the ELSTM-I cell and (b) the ELSTM-II cell.

The ELSTM-I cell can be described by

$$c_t = \sigma(W_f I_t) c_{t-1} + s_t \sigma(W_i I_t) \phi(W_{in} I_t), \quad (20)$$

$$h_t = \sigma(W_o I_t) \phi(c_t + b). \quad (21)$$

where $b \in \mathbb{R}^N$ is a trainable bias vector. The ELSTM-II cell can be written as

$$c_t = c_{t-1} + s_t \sigma(W_i I_t) \phi(W_{in} I_t), \quad (22)$$

$$h_t = \sigma(W_o I_t) \phi(c_t + b). \quad (23)$$

As shown above, we introduce scaling factor, $s_i, i = 1, \dots, t-1$, to the ELSTM-I and the ELSTM-II to increase or decrease the impact of input I_i in the sequence.

To prove that the ELSTM-I has longer memory than the LSTM, we first derive a closed form expression of h_t as

$$h_t = \sigma(W_o I_t) \phi \left(\sum_{k=1}^t s_k \left[\prod_{j=k+1}^t \sigma(W_f I_j) \right] \sigma(W_i I_k) \phi(W_{in} I_k) + b \right). \quad (24)$$

Then, we select s_k such that

$$\left| s_k \prod_{j=k+1}^t \sigma(W_f I_j) \right| \geq \left| \prod_{j=k+1}^t \sigma(W_f I_j) \right|. \quad (25)$$

By comparing Eq. (25) with Eq. (11), we conclude that the ELSTM-I has longer memory than the LSTM. It is important to emphasize that we only need to show the sufficient but not necessary conditions such as those in Eq. (25) to explain the memory capability of an RNN system. In other words, there is no need to argue whether such a system is always capable in retaining longer memory as compared to some other systems. As a matter of fact, retaining longer memory is not always desired, which is the reason why a forgetting gate [12] is introduced for LSTM. On the other hand, if the memory of a RNN model is limited by design, it would have negative impact on its performance.

To examine the memory capability problem from this viewpoint, we find that scaling factors s_k play a role similar to the attention score in various attention models such as Vinyals *et al.* [7]. The impact of proceeding elements to the current output can be adjusted (either increased or decreased) by s_k . The

memory capability of the ELSTM-II can be proven in a similar fashion. We should point out that, even the ELSTM-II does not have a forget gate, it can attend or forget a particular position of a sequence as the ELSTM-I through the scaling factor. On the other hand, fewer parameters are used in the ELSTM-II than the ELSTM-I. The numbers of parameters used by various RNN cells are compared in Table 1, where $X_t \in \mathbb{R}^M$, $h_t \in \mathbb{R}^N$ and $t = 1, \dots, T$.

Table 1: Comparison of Parameter Numbers.

Cell	Number of Parameters
LSTM	$4N(M + N + 1)$
GRU	$3N(M + N + 1)$
ELSTM-I	$4N(M + N + 1) + N(T + 1)$
ELSTM-II	$3N(M + N + 1) + N(T + 1)$

As shown in Table 1, the number of parameters of the ELSTM cell depends on the maximum length, T , of the input sequences, which makes the model size uncontrollable. To address this problem, we choose a fixed T_s (with $T_s < T$) as the upper bound on the number of scaling factors, and set $s_k = s_{(k-1) \bmod T_s + 1}$, if $k > T_s$ and k starts from 1, where mod denotes the modulo operator. In other words, the sequence of scaling factors is a periodic one with period T_s , so the elements in a sequence that are distanced by the length of T_s will share the same scaling factor.

The ELSTM-I cell with periodic scaling factors can be described by

$$c_t = \sigma(W_f I_t) c_{t-1} + s_{t_s} \sigma(W_i I_t) \phi(W_{in} I_t), \quad (26)$$

$$h_t = \sigma(W_o I_t) \phi(c_t + b), \quad (27)$$

where $t_s = (t - 1) \bmod T_s + 1$. Similarly, the ELSTM-II cell with periodic scaling factors can be written as

$$c_t = c_{t-1} + s_{t_s} \sigma(W_i I_t) \phi(W_{in} I_t), \quad (28)$$

$$h_t = \sigma(W_o I_t) \phi(c_t + b). \quad (29)$$

We observe that the choice of T_s affects the network performance. Generally speaking, a small T_s value is suitable for simple language tasks that demand shorter memory while a larger T_s value is desired for complex ones that demand longer memory. For the particular sequence-to-sequence (seq2seq [6, 7]) RNN models, a larger T_s value is always preferred. We will elaborate the parameter settings in Sec. 5.

4. Dependent BRNN (DBRNN) Model

We are interested in the problem of predicting an output sequence, $\{Y_t\}_{t=1}^{T'}$ with $Y_t \in \mathbb{R}^N$, based on an input sequence, $\{X_t\}_{t=1}^T$ with $X_t \in \mathbb{R}^M$, where T and T' are lengths of the input and the output sequences, respectively. To solve this problem, we investigate the macro RNN model and propose a multi-task model, called the dependent BRNN (DBRNN), in this section. Our design is inspired by pros and cons of two RNN models; namely, the bidirectional RNN (BRNN) [5] and the encoder-decoder design [4]. We will review the BRNN and the encoder-decoder in Sec. 4.1 and, then, propose the DBRNN in Sec. 4.2 in this section.

4.1. BRNN and Encoder-Decoder

The BRNN is used to model the conditional probability density function in form of

$$P(Y_t|\{X_i\}_{i=1}^T).$$

Its output is a combination of the output of a forward RNN and the output of a backward RNN. Due to the bidirectional design, the BRNN can utilize the information of the entire input sequence to predict each individual output element. However, the BRNN does not exploit the predicted output in predicting Y_t , and elements in the predicted sequence

$$\hat{Y}_t = \operatorname{argmax}_{Y_t} P(Y_t|\{X_i\}_{i=1}^T)$$

are generated from the input sequences only. Since the prediction of each individual output is conducted independently, the inherent correlation among

elements in the output sequence is not utilized during the prediction stage. The correlation can be maximally captured by explicitly feeding the previous predicted outputs back to the system to avoid the mis-alignment [8] problem. This idea is exploited by the encoder-decoder system in form of

$$\hat{Y}_t = \operatorname{argmax}_{Y_t} P(Y_t | \{\hat{Y}_i\}_{i=1}^{t-1}, \{X_i\}_{i=1}^T).$$

On the other hand, the encoder-decoder system is vulnerable to previous erroneous predictions in the forward path. Recently, the BRNN was introduced to the encoder by Bahdanau *et al.* [8], yet their design does not address the erroneous prediction problem.

4.2. DBRNN Model and Training

Being motivated by observations in Sec. 4.1, we propose a multi-task BRNN model, called the dependent BRNN (DBRNN), to achieve the following objectives:

$$p_t = W^f p_t^f + W^b p_t^b \quad (30)$$

$$\hat{Y}_t^f = \operatorname{argmax}_{Y_t} p_t^f, \quad (31)$$

$$\hat{Y}_t^b = \operatorname{argmax}_{Y_t} p_t^b, \quad (32)$$

$$\hat{Y}_t = \operatorname{argmax}_{Y_t} p_t \quad (33)$$

where

$$p_t^f = P(Y_t | \{X_i\}_{i=1}^T, \{\hat{Y}_i^f\}_{i=1}^t), \quad (34)$$

$$p_t^b = P(Y_t | \{X_i\}_{i=1}^T, \{\hat{Y}_i^b\}_{i=t}^{T'}), \quad (35)$$

$$p_t = P(Y_t | \{X_i\}_{i=1}^T), \quad (36)$$

and W^f and W^b are trainable weights. As shown in Eqs. (31), (32) and (33), the DBRNN has three learning objectives: 1) the target sequence for the forward RNN prediction, 2) the reversed target sequence for the backward RNN prediction, and 3) the target sequence for the bidirectional prediction.

The DBRNN model is shown in Fig. 3. It consists of a lower and an upper BRNN branches. At each time step, the input to the forward and the backward parts of the upper BRNN is the concatenated forward and backward outputs from the lower BRNN branch. The final bidirectional prediction is the pooling of both the forward and the backward predictions. We will show later that this design will make the DBRNN robust to previous erroneous predictions.

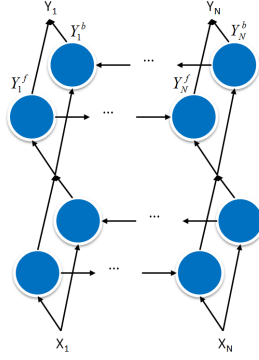


Figure 3: The DBRNN model.

Let $F(\cdot)$ be the cell function. The input is fed into the forward and backward RNN of the lower BRNN branch as

$$h_t^f = F_l^f(x_t, c_{l(t-1)}^f), \quad h_t^b = F_l^b(x_t, c_{l(t+1)}^b), \quad h_t = \begin{bmatrix} h_t^f \\ h_t^b \end{bmatrix}, \quad (37)$$

where c and l denote the cell hidden state and the lower BRNN, respectively. The final output, h_t , of the lower BRNN is the concatenation of the output, h_t^f , of the forward RNN and the output, h_t^b , of the backward RNN. Similarly, the upper BRNN generates the final output p_t as

$$p_t^f = F_u^f(h_t, c_{u(t-1)}^f), \quad p_t^b = F_u^b(h_t, c_{u(t+1)}^b), \quad p_t = W^f p_t^f + W^b p_t^b, \quad (38)$$

where u denotes the upper BRNN. To generate forward prediction \hat{Y}_t^f and backward prediction \hat{Y}_t^b , the forward and backward paths of the upper BRNN branch are separately trained by the original and the reversed target sequences, respectively. The results of forward and backward predictions of the upper RNN branch are then combined to generate the final result.

There are three errors: 1) forward prediction error e_f for \hat{Y}_t^f , 2) backward prediction error e_b for \hat{Y}_t^b , and 3) bidirectional prediction error e for \hat{Y}_t . To train the proposed DBRNN, e_f is backpropagated through time to the upper forward RNN and the lower BRNN, e_b is backpropagated through time to the upper backward RNN and the lower BRNN, and e is backpropagated through time to the entire model.

To show that DBRNN is more robust to previous erroneous predictions than one-directional models, we compare their cross entropy defined as

$$l = - \sum_{k=1}^K p_{t,k} \log(\hat{p}_{t,k}), \quad (39)$$

where K is the total number of classes (e.g. the size of vocabulary for the language task), \hat{p}_t is the predicted distribution, and p_t is the ground truth distribution with k' as the ground truth label. It is in form of one-hot vector. That is,

$$p_t = (\delta_{1,k}, \dots, \delta_{k,k'}, \dots, \delta_{K,k})^T, \quad k = 1, \dots, K,$$

where $\delta_{k,k'}$ is the Kronecker delta function. Based on Eq. (30), l can be further expressed as

$$l = - \sum_{k=1}^K p_{t,k} \log(W_k^f \hat{p}_{t,k}^f + W_k^b \hat{p}_{t,k}^b), \quad (40)$$

$$= - \log(W_{k'}^f \hat{p}_{t,k'}^f + W_{k'}^b \hat{p}_{t,k'}^b). \quad (41)$$

We can select $W_{k'}^f$ and $W_{k'}^b$ such that $W_{k'}^f \hat{p}_{t,k'}^f + W_{k'}^b \hat{p}_{t,k'}^b$ is greater than $\hat{p}_{t,k'}^f$ and $\hat{p}_{t,k'}^b$. Then, we obtain

$$l < - \sum_{k=1}^K \log(\hat{p}_{tk}^f), \quad (42)$$

$$l < - \sum_{k=1}^K \log(\hat{p}_{tk}^b). \quad (43)$$

The above two equations indicate that the DBRNN can have a cross entropy lower than those of one-directional predictions by pooling opinions from both the forward and the backward predictions.

It is worthwhile to compare the proposed DBRNN and the bi-attention model in Cheng *et al.* [13]. Both of them have bidirectional predictions for the output, yet there are three main differences. First, the DBRNN provides a generic solution to the SISO problem without being restricted to dependency parsing. The target sequences in training (namely, \hat{Y}_t^f , \hat{Y}_t^b and \hat{Y}_t) are the same for the DBRNN while the solution in [13] has different target sequences. Second, the attention mechanism is used in [13] but not in the DBRNN. Third, The encoder-decoder design is adopted by [13] but not by the DBRNN.

5. Experiments

5.1. Experimental Setup

In the experiments, we compare the performance of five RNN macro-models:

1. basic one-directional RNN (basic RNN);
2. bidirectional RNN (BRNN);
3. sequence-to-sequence (seq2seq) RNN [6] (a variant of the encoder-decoder);
4. seq2seq with attention [7];
5. dependent bidirectional RNN (DBRNN), which is proposed in this work.

For each RNN model, we compare four cell designs: LSTM, GRU, ELSTM-I and ELSTM-II.

We conduct experiments on two problems: part of speech (POS) tagging and dependency parsing (DP). We report the testing accuracy for the POS tagging problem and the unlabeled attachment score (UAS) and the labeled attachment score (LAS) for the DP problem. The POS tagging task is an easy one which requires shorter memory while the DP task demands much longer memory. For the latter, there exist more complex relations between the input and the output. For the DP problem, we compare our solution with the GRU-based bi-attention model (bi-Att). Furthermore, we compare the DBRNN using the ELSTM cell with two other non-RNN-based neural network methods. One is transition-based DP with neural network (TDP) proposed by Chen *et al.* [14]. The other

is convolutional seq2seq (ConvSeq2seq) proposed by Gehring *et al.* [15]. For the proposed DBRNN, we show the best results from the three outputs (namely, p_t^f , p_t^b and p_t). We adopt $T_s = 1$ in the basic RNN, BRNN, and DBRNN models and $T_s = 100$ in the other two seq2seq models for the POS tagging problem. We use $T_s = 100$ in all models for the DP problem.

The training dataset used for both problems are from the Universal Dependency 2.0 English branch (UD-English). It contains 12,543 sentences and 14,985 unique tokens. The test dataset in both experiments is from the test English branch (gold, en.conllu) of CoNLL 2017 shared task development and test data. The input to the POS tagging and the DP problems are the stemmed and lemmatized sequences (column 3 in CoNLL-U format). The target sequence for the POS tagging is the universal POS tag (column 4). The target sequence for the DP is the interleaved dependency relation to the headword (relation, column 8) and its headword position (column 7). As a result, the length of the target sequence for the DP is twice of the length of the input sequence.

Table 2: Network parameters and training details.

Number of RNN layers	1
Embedding layer vector size	512
Number of RNN cells	512
Batch size	20
Training steps	11 epochs
Learning rate	0.5
Optimizer	AdaGrad[16]

The input is first fed into a trainable embedding layer [17] before it is sent to the actual network. Table 2 shows the detailed network and training specifications. We do not finetune network hyper-parameters or apply any engineering trick (e.g. feeding additional inputs other than the raw embedded input sequences) for the best possible performance since our main goal is to compare the performance of the LSTM, GRU, ELSTM-I and ELSTM-II cells under var-

ious macro-models.

Table 3: POS tagging test accuracy (%)

	LSTM	GRU	ELSTM-I	ELSTM-II
BASIC RNN	87.30	87.51	87.44	86.92
BRNN	89.55	89.39	89.29	86.89
Seq2seq	24.43	35.27	50.42	57.84
Seq2seq with Att	31.34	34.60	81.72	57.35
DBRNN	89.86	89.06	89.28	87.97

Table 4: DP test results (UAS/LAS %)

	LSTM	GRU	ELSTM-I	ELSTM-II
BASIC RNN	43.24/25.28	45.24/29.92	58.49/36.10	58.87/36.50
BRNN	37.88/25.26	16.86/8.95	55.97/35.13	52.15/31.72
Seq2seq	29.38/6.05	36.47/13.44	48.58/24.05	53.84/34.08
Seq2seq with Att	31.82/16.16	43.63/33.98	64.30/52.60	55.13/35.60
DBRNN	52.19/40.29	52.23/37.25	61.35/ 43.32	61.94/42.89
Bi-Att [13] ¹		59.97/44.94		

5.2. Comparison of RNN Models

The results of the POS tagging and the DP problems are shown in Tables 3 and 4, respectively. We see that the DBRNN outperforms the BRNN and the seq2seq in both the POS tagging and the DP problems regardless of the cell types. This shows the advantage of expert opinion pooling from the input as well as the predicted output. The DBRNN achieves a training loss that is similar or better than the seq2seq model with attention as shown in Figs. 4 and 5. However, the DBRNN can overfit to the training data more easily due to a

¹The result is generated by using exactly the same settings in Table. 2. We do not feed in the network with information other than input sequence itself.

larger model size. To overcome it, one can use a proper regularization scheme in the training process.

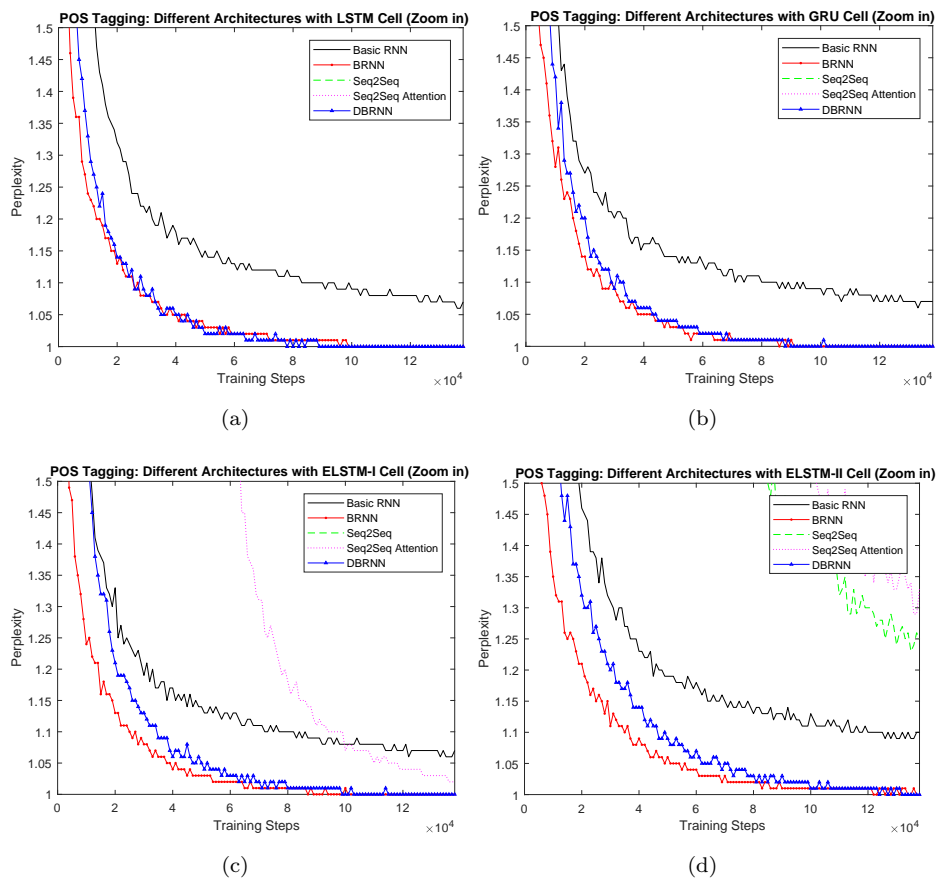


Figure 4: The training perplexity of different models with the LSTM (top left), the GRU (top right), the ELSTM-I (bottom left) and the ELSTM-II (bottom right) for the POS tagging task.

The proposed ELSTM-I and ELSTM-II cells outperform the LSTM and GRU cells in most RNN models. This is especially true for complex language tasks, where the two ELSTM cells outperform traditional cell designs by a significant margin. This demonstrates the effectiveness of the sequence of scaling factors adopted by the ELSTM cells. It allows the network to retain longer memory with better attention.

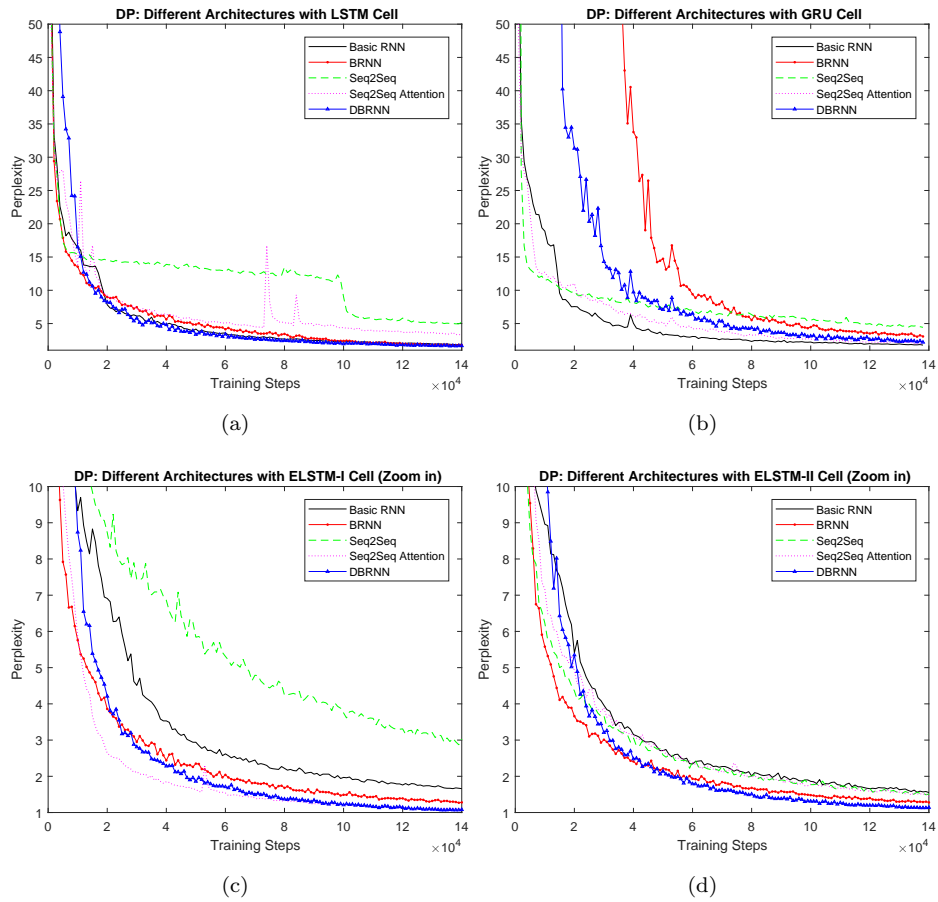


Figure 5: The training perplexity of different models with the LSTM (top left), the GRU (top right), the ELSTM-I (bottom left) and the ELSTM-II (bottom right) cells for the DP task.

The ELSTM-I cell even outperforms the bi-Att model, which was designed specifically for the DP task. For the POS tagging problem, the advantage of the ELSTM cells is not as obvious. This is probably due to the shorter memory requirement in this simple task. In this context, ELSTM cells are over-parameterized, and they converge slower and tend to overfit the training data.

The ELSTM-I and ELSTM-II cells with large T_s value perform particularly well for the seq2seq (with and without attention) model. The hidden state, c_t , of ELSTM cells is more expressive in representing patterns over a longer distance. Since the seq2seq design relies on the expressive power of a hidden state, ELSTMs have a clear advantage.

To substantiate our claim in Sec. 2, we conduct additional experiments to show the robustness of the ELSTM cells and the DBRNN. Specifically, we compare the performance of the same five models with LSTM, ELSTM-I and ELSTM-II with $I_t = X_t$ for the same language tasks. We do not include the GRU cell since it inherently demands $I_t^T = [X_t^T, h_{t-1}^T]$. The convergence behaviors of $I_t = X_t$ and $I_t^T = [X_t^T, h_{t-1}^T]$ with the LSTM, ELSTM-I and ELSTM-II cells for the DP problem are shown in Fig. 6. We see that the ELSTM-I and the ELSTM-II do not behave much differently between $I_t = X_t$ and $I_t^T = [X_t^T, h_{t-1}^T]$ while the LSTM does. This shows the effectiveness of the ELSTM-I and the ELSTM-II design regardless of the input. More performance comparison will be provided in the Appendix.

5.3. Comparison between ELSTM and Non-RNN-based Methods

As stated earlier, the ELSTM design is more capable of extending the memory and capturing complex SISO relationships than other RNN cells. In this subsection, we compare the DP performance of two models built upon the ELSTM-I cell (namely, the DBRNN and the seq2seq with attention) and two non-RNN-based neural network based methods (i.e., the TDP [14] and the convseq2seq [15]). The TDP is a hand-crafted method based on a parsing tree, and its neural network is a multi-layer perceptron with one hidden layer. Its neural network is

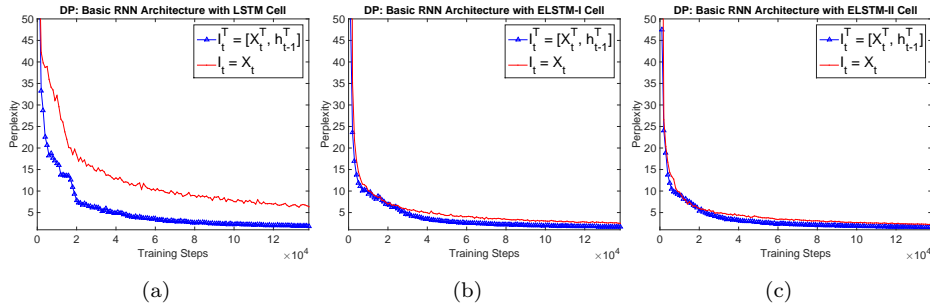


Figure 6: Training perplexity of the basic RNN with $I_t = X_t$ and $I_t^T = [X_t^T, h_{t-1}^T]$ for the DP problem.

used to predict the transition from a tail word to its headword. The convseq2seq is an end-to-end convolutional neural network (CNN) with an attention mechanism. We used the default settings for the TDP and the convseq2seq as reported in [14] and [15], respectively. For the TDP, we do not use the ground truth POS tags but the predicted dependency relation labels as the input to the parsing tree for the next prediction.

We see from Table 5 that the ELSTM-based models learn much faster than the CNN-based convseq2seq model with fewer parameters. The convseq2seq uses dropout while the ELSTM-based models do not. It is also observed that convseq2seq does not converge if Adagrad is used as its optimizer. The ELSTM-I-based seq2seq with attention even outperforms the TDP, which was specifically designed for the DP task. Without a good pretrained word embedding scheme, the UAS and LAS of TDP drop drastically to merely 8.93% and 0.30% respectively.

6. Conclusion and Future Work

Although the memory of the LSTM and GRU cells fades slower than that of the SRN, it is still not long enough for complicated language tasks such as dependency parsing. To address this issue, we proposed the ELSTM-I and the ELSTM-II to enhance the memory capability of an RNN cell. Besides, we

Table 5: DP test accuracy (%) and system settings

	Seq2seq-E-I	DBRNN-E-II	Convseq2seq	TDP
UAS	64.30	61.94	52.55	62.29
LAS	52.60	42.89	44.19	52.18
Training steps	11 epochs	11 epochs	11 epochs	11 epochs
# parameters	12,684,468	16,460,468	22,547,124	950,555
Pretrained embedding	No	No	No	Yes
End-to-end	Yes	Yes	Yes	No
Regularization	No	No	No	Yes
Dropout	No	No	Yes	Yes
Optimizer	AdaGrad	AdaGrad	NAG [18]	AdaGrad
Learning rate	0.5	0.5	0.25	0.01
Embedding size	512	512	512	50
Encoder layers	1	N/A	4	N/A
Decoder layers	1	N/A	4	N/A
Kernel size	N/A	N/A	3	N/A
Hidden layer size	N/A	N/A	N/A	200

presented a new DBRNN model that has the merits of both the BRNN and the encoder-decoder. It was shown by experimental results that the ELSTM-I and the ELSTM-II outperforms other RNN cell designs by a significant margin for complex language tasks. The DBRNN model is superior to the BRNN and the seq2seq models for simple and complex language tasks. Furthermore, the ELSTM-based RNN models outperform the CNN-based convseq2seq model and the handcrafted TDP. There are interesting issues to be explored furthermore. For example, is the ELSTM cell also helpful in more sophisticated RNN models such as the deep RNN? Is it possible to make the DBRNN deeper and better? They are left for future study.

7. Declarations of interest

Declarations of interest: none

8. Acknowledgements

This research did not receive any specific grant from funding agencies in the public, commercial, or not-for-profit sectors.

References

References

- [1] J. Elman, Finding structure in time, *Cognitive Science* 14 (1990) 179–211.
- [2] M. Jordan, Serial order: A parallel distributed processing approach, *Advances in Psychology* 121 (1997) 471–495.
- [3] S. Hochreiter, J. Schmidhuber, Long short-term memory, *Neural Computation* 9 (1997) 1735–1780.
- [4] K. Cho, B. v. Merriënboer, C. Gulcehre, D. Bahdanau, F. Bougares, H. Schwenk, Y. Bengio, Learning phrase representations using RNN encoderdecoder for statistical machine translation, In *Proceedings of The Empirical Methods in Natural Language Processing (EMNLP 2014)*.

- [5] M. Schuster, K. K. Paliwal, Bidirectional recurrent neural networks, *Signal Processing* 45 (1997) 2673–2681.
- [6] I. Sutskever, O. Vinyals, Q. V. Le, Sequence to sequence learning with neural networks, *Advances in Neural Information Processing Systems* (2014) 3104–3112.
- [7] O. Vinyals, L. Kaiser, T. Koo, S. Petrov, I. Sutskever, G. Hinton, Grammar as a foreign language, *Advances in Neural Information Processing Systems* (2015) 2773–2781.
- [8] D. Bahdanau, K. Cho, Y. Bengio, Neural machine translation by jointly learning to align and translate, In *Proceedings of the International Conference on Learning Representations (ICLR 2015)*.
- [9] R. Pascanu, C. Gulcehre, K. Cho, Y. Bengio, How to construct deep recurrent neural networks, [arXiv:1312.6026](https://arxiv.org/abs/1312.6026).
- [10] P. Razvan, T. Mikolov, Y. Bengio, On the difficulty of training recurrent neural networks, In *Proceedings of The International Conference on Machine Learning (ICML 2013)* (2013) 1310–1318.
- [11] Y. Bengio, P. Simard, P. Frasconi, Learning long-term dependencies with gradient descent is difficult, *Neural Networks* 5 (1994) 157–166.
- [12] F. A. Gers, J. Schmidhuber, F. Cummins, Learning to forget: Continual prediction with lstm, *Neural Computation* (2000) 2451–2471.
- [13] H. Cheng, H. Fang, X. He, J. Gao, L. Deng, Bi-directional attention with agreement for dependency parsing, In *Proceedings of The Empirical Methods in Natural Language Processing (EMNLP 2016)*.
- [14] D. Chen, M. Christopher, A fast and accurate dependency parser using neural networks, in: *In Proceedings of The Empirical Methods in Natural Language Processing (EMNLP 2014)*, 2014, pp. 740–750.

- [15] J. Gehring, G. Auli M, D. Yarats, Y. Denis, D. Yann N., Convolutional sequence to sequence learning, in: arXiv preprint, no. 1705.03122, 2017.
- [16] Duchi, Adaptive subgradient methods for online learning and stochastic optimization, *The Journal of Machine Learning Research* (2011) 2121–2159.
- [17] Y. Bengio, R. Ducharme, P. Vincent, C. Jauvin, A neural probabilistic language model, *Journal of Machine Learning Research* (2003) 1137–1155.
- [18] Y. Nesterov, A method of solving a convex programming problem with convergence rate $o(1/k^2)$, in: *Soviet Mathematics Doklady*, Vol. 27, 1983, pp. 372–376.

Appendix A: More Experimental Results

In the appendix, we provide more experimental results to shed light on the convergence performance in the training of various models with different cells for the POS tagging and the DP tasks. First, we compare the training perplexity between $I_t = X_t$ and $I_t^T = [X_t^T, h_{t-1}^T]$ for various models with the LSTM, the ELSTM-I and the ELSTM-II cells in Figs. .7-12. Then, we examine the training perplexity with $I_t^T = [X_t^T, h_{t-1}^T]$ for various models with different cells in Figs. .13-15.

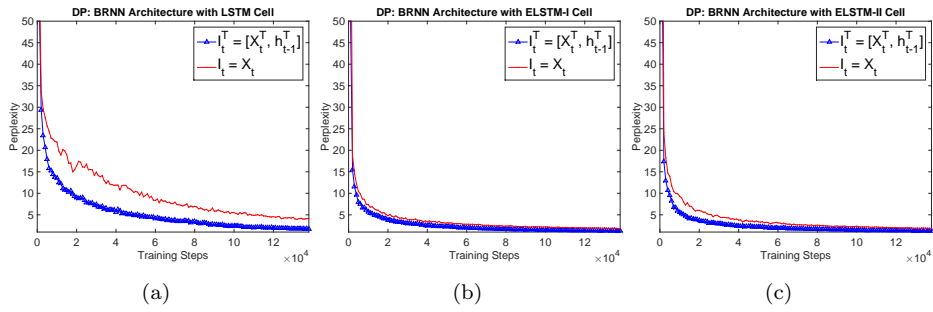


Figure .7: The training perplexity of the BRNN model with $I_t = X_t$ and $I_t^T = [X_t^T, h_{t-1}^T]$ for the DP task.

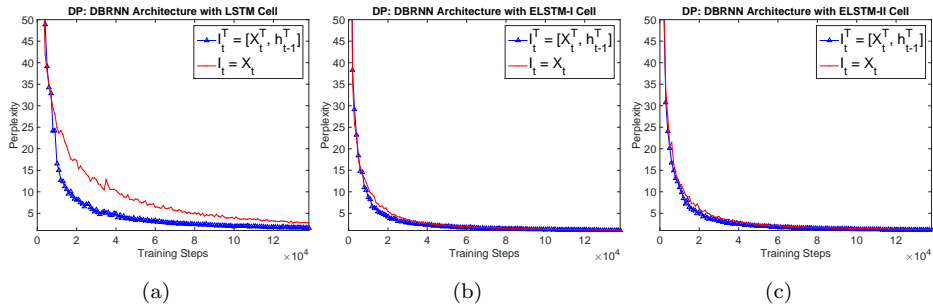


Figure .8: The training perplexity of the DBRNN model with $I_t = X_t$ and $I_t^T = [X_t^T, h_{t-1}^T]$ for the DP task.

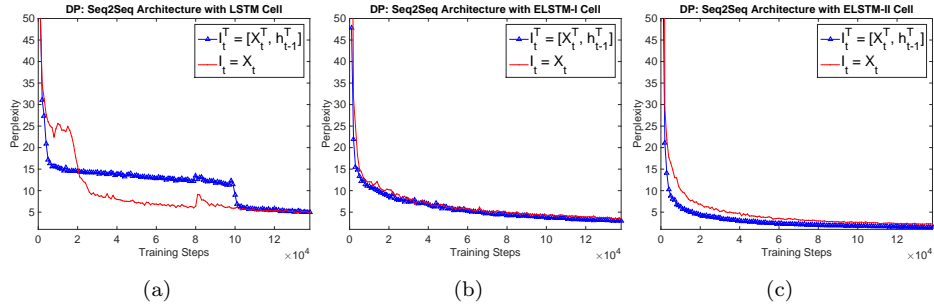


Figure .9: The training perplexity of the seq2seq model with $I_t = X_t$ and $I_t^T = [X_t^T, h_{t-1}^T]$ for the DP task.

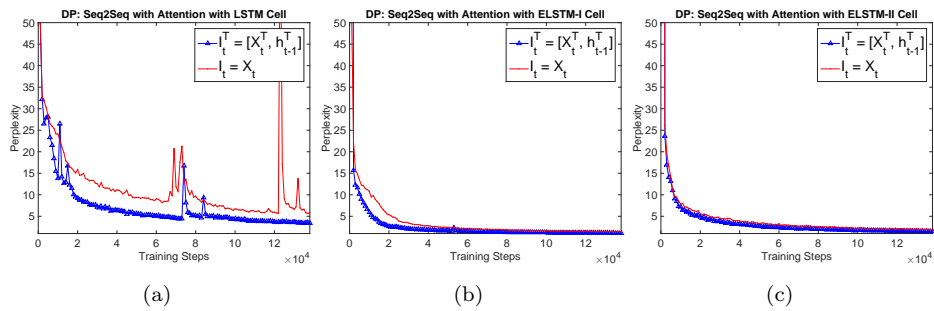


Figure .10: The training perplexity of the seq2seq with attention model with $I_t = X_t$ and $I_t^T = [X_t^T, h_{t-1}^T]$ for the DP task.

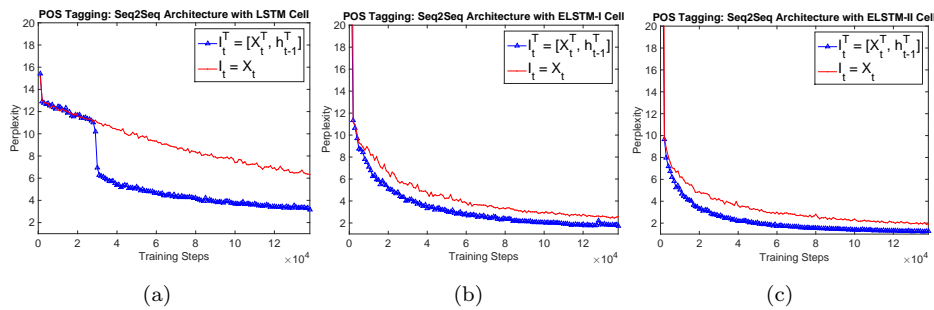


Figure .11: The training perplexity of the seq2seq model with $I_t = X_t$ and $I_t^T = [X_t^T, h_{t-1}^T]$ for the POS tagging task.

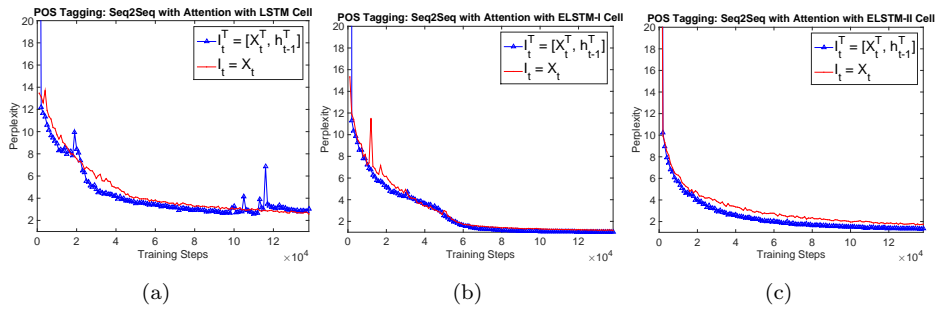


Figure .12: The training perplexity of the seq2seq with Att model with $I_t = X_t$ and $I_t^T = [X_t^T, h_{t-1}^T]$ for the POS tagging task.

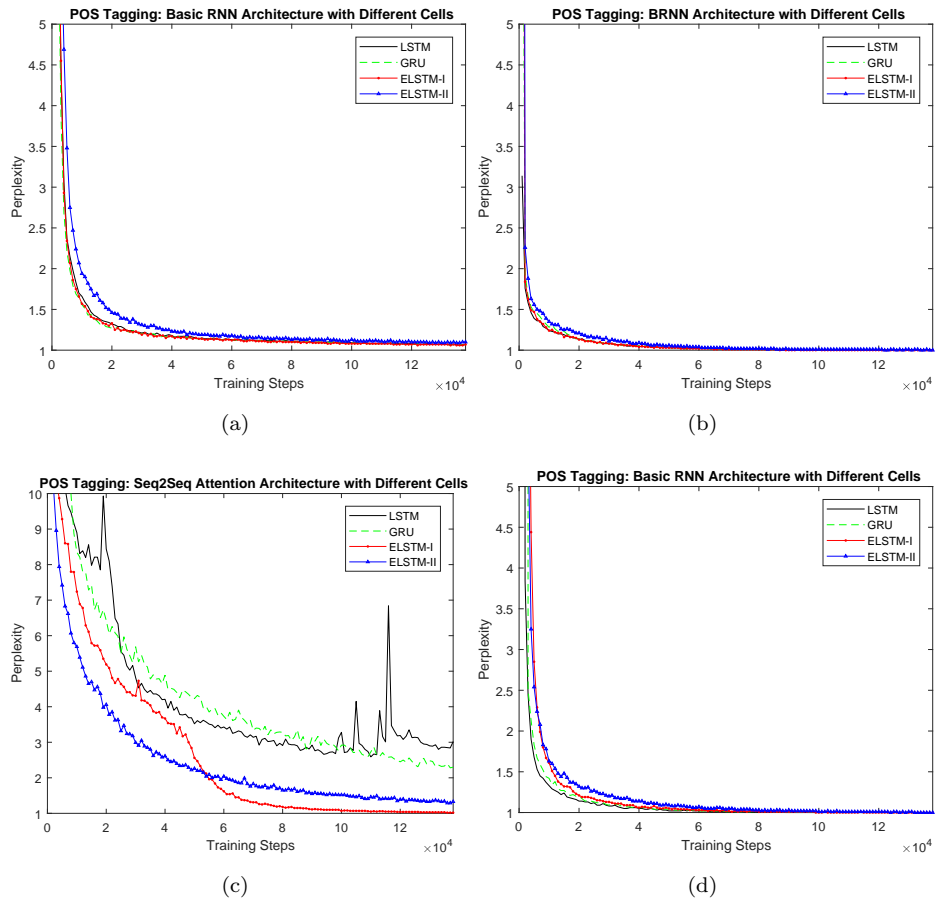


Figure .13: The training perplexity for the basic RNN (top left), the BRNN (top right), the seq2seq with Att (bottom left) and the DBRNN (bottom right) for the POS tagging.

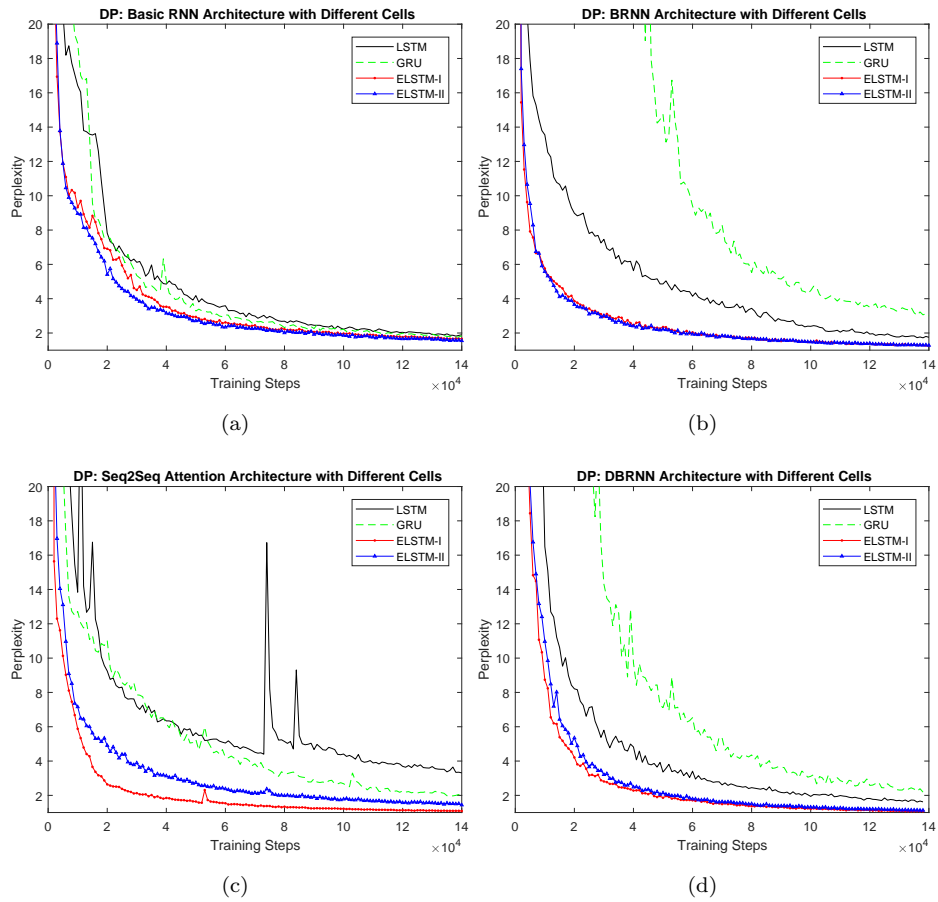


Figure .14: The training perplexity for the basic RNN (top left), the BRNN (top right), the seq2seq with Att (bottom left) and the DBRNN models (bottom right) for the DP task.

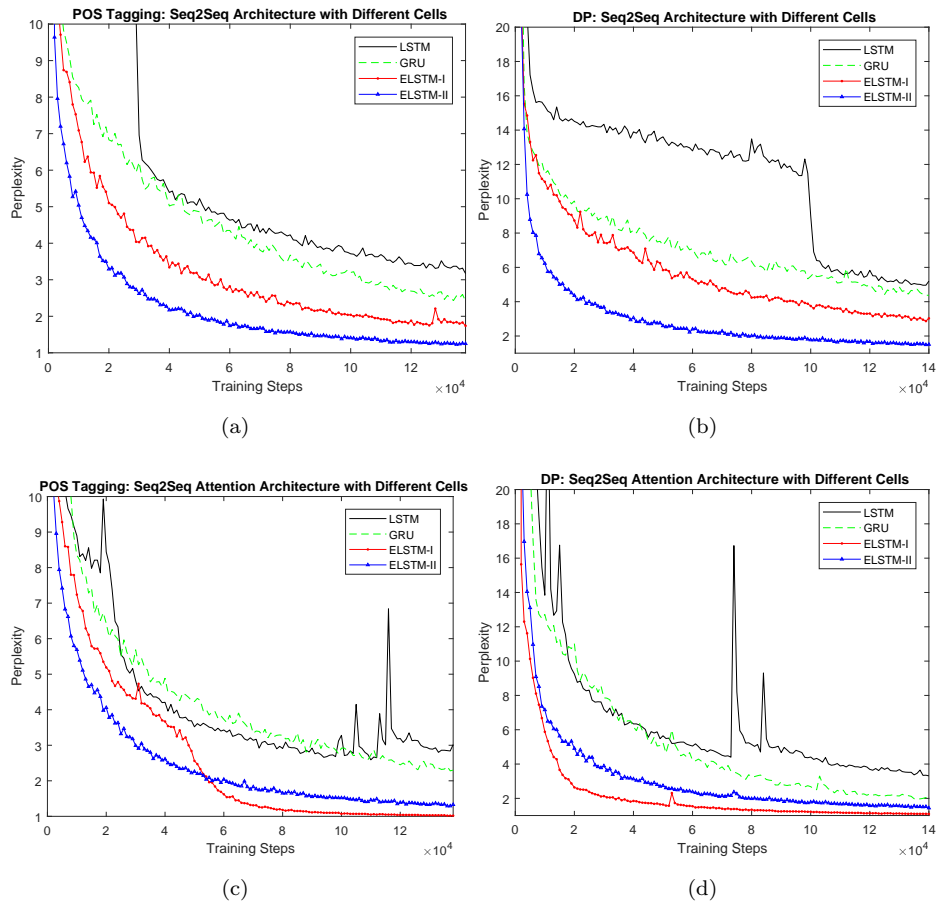


Figure .15: The training perplexity for the seq2seq model (top), and the seq2seq with Att model (bottom), for the POS task (left) and the DP (right) task.